

Applications of Electromagnetically Induced Transparency to Quantum Information Processing

R. G. Beausoleil,^{1,*} W. J. Munro,² D. A. Rodrigues,² and T. P. Spiller²

¹*Hewlett-Packard Laboratories, 13837 175th Pl. NE, Redmond, WA 98052-2180, USA*

²*Hewlett-Packard Laboratories, Filton Road, Stoke Gifford, Bristol BS34 8QZ, United Kingdom*

(Dated: February 15, 2004)

We provide a broad outline of the requirements that should be met by components produced for a Quantum Information Technology (QIT) industry, and we identify electromagnetically induced transparency (EIT) as potentially key enabling science toward the goal of providing widely available few-qubit quantum information processing within the next decade. As a concrete example, we build on earlier work and discuss the implementation of a two-photon controlled phase gate (and, briefly, a one-photon phase gate) using the approximate Kerr nonlinearity provided by EIT. In this paper, we rigorously analyze the dependence of the performance of these gates on atomic dephasing and field detuning and intensity, and we calculate the optimum parameters needed to apply a π phase shift in a gate of a given fidelity. Although high-fidelity gate operation will be difficult to achieve with realistic system dephasing rates, the moderate fidelities that we believe will be needed for few-qubit QIT seem much more obtainable.

PACS numbers: 42.50.-p, 85.60.Gz, 32.80.-t, 03.67.-a, 03.67.Lx

INTRODUCTION

Quantum Information Science (QIS)[1] is a rapidly emerging discipline with the potential to revolutionize measurement, computation and communication. Sitting at the intersection of quantum electronics, quantum optics, and information theory, QIS offers a new paradigm for the collection, transmission, reception, storage and processing of information, based on the laws of quantum, rather than classical, physics. Applications of QIS certainly have the potential to generate totally new Quantum Information Technology (QIT), but ultimately any future QIT industry will be justified by commercial interest in the products and services that it supports. Practical results in QIS are currently right at the cutting edge of experimental quantum research, so the route to QIT is very hard going. From the commercial perspective, a major challenge is the creation of relatively simple QIT which is nevertheless economically viable. This would generate revenue and expand current industrial participation and interest in the field, effectively seeding a new QIT industry, in the same way hearing aids were the first commercial application of the transistor and the beginning of the classical IT industry.

A long term goal for QIT is the realization of many-qubit scalable quantum processors. It is known that these machines would outperform their classical counterparts at certain tasks such as factoring[2] and searching,[3] and the search continues for new applications. A shorter term goal is the realization of (say) 50-100 qubit processors. These would certainly be better at quantum simulation[4] than any foreseeable conventional IT and, as a research tool, would expose QIT to a whole new class of curious and creative people, with all their potential for new ideas and applications. However, perhaps the most immediate QIT, that which will stimulate a new industry, is based on or related to quantum communication[5] and metrology.[6]

It has become clear over the last two decades that computer and network security that relies primarily on software protocols is potentially porous, being based on unproven mathematical assumptions. In QIS, quantum computation and communication protocols can be devised in which unconditional privacy is guaranteed by fundamental laws of physics. Although it is not clear yet that quantum key distribution (QKD) will be the first profitable application of QIT, it is possible that extensions of QKD (e.g., controlled entanglement swapping), photonic state comparison (for quantum signature verification), and full quantum communication at high data rates will become compelling to financial, medical, and other institutions and their customers. Furthermore, it is already clear that distributed quantum algorithms can efficiently enable solutions to economics problems (e.g., public goods economics[7]) that are difficult to treat with conventional mechanisms, but it is not yet known whether other economic procedures—such as auctions—have superior quantum solutions. Similarly, quantum metrology and imaging have interest for the nanoscale manufacturing and physical security industries, as these techniques allow tiny phase shifts, displacements, and forces to be accurately measured remotely even when the target is enclosed within an inaccessible or hostile environment.

Although there are still open questions, one promising route for starting a QIT industry is to found it on communication and metrology applications, based on the generation, transmission, processing, and detection of a few photonic qubits. It is certainly clear that photons (or other quantum states of light) are *the* qubits of choice for

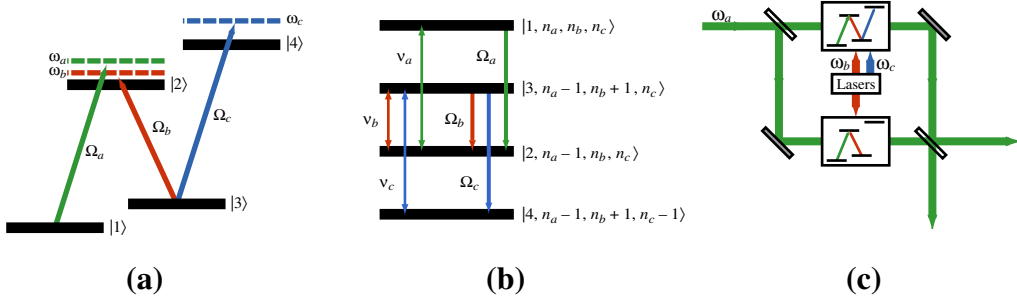


FIG. 1: Electric dipole interaction between a four-level \mathcal{N} atom and a nearly resonant three-frequency electromagnetic field. (a) In the semiclassical view, two atomic energy levels are separated by the energy $\hbar\omega_{ij}$, and coupled by a field oscillating at the frequency $\omega_k = \omega_{ij} + \nu_k$. The strength and phase of the corresponding dipole interaction is represented by the Rabi frequency $\Omega_k \propto \sqrt{n_k}$. (b) In the quantum view, the states of the atom + photons system separate into manifolds coupled internally by resonant transitions. (c) A model Mach-Zehnder interferometer illustrating an architecture for a “dual rail” quantum phase-shifter using four-level \mathcal{N} atoms. The upper arm is denoted by “1” and the lower arm by “0.”

communication,[5] and so for few-qubit processing there is a case for keeping everything optical. It is also the case that potentially useful processing tasks could be performed with moderate (10–20%) gate error rates, rather larger than the stricter error bounds demanded for fault-tolerant many-qubit processing. This “all optical” scenario is the motivation for our work. Clearly, taking this approach, quantum information processing primitives based on nonlinear quantum optics (such as a universal set of optical gates and single-photon detectors) must be developed and fabricated. These primitives would potentially allow the construction of few-qubit nanoscale quantum optical processors that could be incorporated into existing PCs and communication networks. In this paper we discuss the possibility of realizing these primitives through use of electromagnetically induced transparency (EIT).

ELECTROMAGNETICALLY INDUCED TRANSPARENCY

In previous work,[8] we considered a model of the nonlinear electric dipole interaction between three quantum electromagnetic radiation fields with angular frequencies ω_a , ω_b , ω_c and a corresponding four-level \mathcal{N} atomic system, as shown in Fig. 1(a). We considered N atoms, fixed and stationary in a volume that is small compared to the optical wavelengths, and we assumed that the three frequency channels of the resonant four-level manifold of the resulting quantum system shown in Fig. 1(b) are driven by Fock states containing n_a , n_b , and n_c photons, corresponding to the Rabi frequencies Ω_a , Ω_b , and Ω_c , respectively. As an example of the use of an EIT system as a phase-shifter, we incorporate the atomic system into the dual-rail Mach-Zehnder interferometer shown in Fig. 1(c). We wish to apply a phase shift to the photon in mode a on the upper rail, conditioned on the presence of one or more photons in mode c . In one arm of the interferometer, the four-level atoms are prepared using $|\Omega_c| > 0$ to provide a phase shift at the probe frequency ω_a while remaining largely transparent and dispersive. In the second arm, $|\Omega_c| = 0$, and the system is tuned to match the absorption and dispersion provided by the atoms in the first arm, allowing the interferometer to remain time-synchronous.

We must be careful to demonstrate that the interaction of either arm with a photon at the probe frequency that has entered the interferometer at the input port will entangle the optical modes with each other but *not* with either collection of atoms. Therefore, we solve the density matrix equation of motion in the presence of a completely general Lindblad damping model, and monitor the element $\rho_{10}(t)$ that corresponds to the initial (ground) state of the entire collection of atoms in both ensembles. If the field in mode b is indeed described by a Fock state, then using the quasi-steady-state approximation[10] ($|\Omega_a| \lesssim \gamma_{20}$) we obtain[8]

$$\rho_{10}(t) \cong \rho_{10}(0) e^{(-\gamma_{10} + iW_{10})Nt}, \quad (1)$$

where the Rabi frequencies Ω_k and detunings ν_k are defined in Fig. 1(a) and (b), and

$$W_{10} \equiv -\frac{\left[(\nu_a - \nu_b + i\gamma_{30})(\nu_a - \nu_b + \nu_c + i\gamma_{40}) - |\Omega_c|^2 \right] |\Omega_a|^2}{(\nu_a + i\gamma_{20}) \left[(\nu_a - \nu_b + i\gamma_{30})(\nu_a - \nu_b + \nu_c + i\gamma_{40}) - |\Omega_c|^2 \right] - (\nu_a - \nu_b + \nu_c + i\gamma_{40}) |\Omega_b|^2}. \quad (2)$$

The constant $\gamma_{j0}, j \in \{2, 3, 4\}$ represents the net decoherence rate (depopulation + dephasing) of level j of the quantum manifold shown in Fig. 1(b) for the atom + field system on the first rail relative to the evolution of a system (absent mode c) on the second rail, while γ_{10} represents the decoherence rate of the collective ground state divided by the number of atoms N . Since the atomic levels $|1\rangle$ and $|3\rangle$ are metastable by assumption, the decoherence rates γ_{10} and γ_{30} represent pure dephasing mechanisms.

TWO-QUBIT PHASE GATES

Suppose that we consider the concrete case of a phase gate that couples single photons in modes a and c and is driven by a coherent state in mode b . We wish to optimize the experimentally controllable parameters so that we introduce a phase shift between the two arms of the system with minimum error. We proceed by choosing *a priori* an error δ which occurs over the entire gate operation, and determining the parameters needed for the gate to perform with this level of error. There will be three sources of error: the dephasing described by γ_{10} and γ_{30} ; the additional depopulation described by γ_{20} and γ_{40} ; and the error arising from the finite value of α_b for the coherent state in mode b , which prevents the system from evolving to a perfect phase-shifted state even in the absence of decoherence.

Suppose that a phase shift of $-\phi \equiv \text{Re}(W_{10})Nt$ is applied by the phase gate after a time t . Then the density matrix element given by Eq. (1) can be rewritten as $\rho_{10}(t) = \rho_{10}(0)e^{-i\phi}e^{-\tau_{\text{eff}}}$, where the effective decoherence time τ_{eff} is defined as

$$\tau_{\text{eff}} \equiv -\frac{\gamma_{10} + \text{Im}(W_{10})}{\text{Re}(W_{10})}\phi. \quad (3)$$

For a given gate fidelity F (a measure of the distance between the ideal output state of the gate and the state that is actually generated[1, 8]), the net error $\delta \equiv 1 - F^2$ due to dephasing and depopulation is $|\rho_{10}(0)|^2(1 - e^{-2\tau_{\text{eff}}}) \approx \tau_{\text{eff}}/2$. In the absence of significant dephasing, it is clear that a large value of the detuning ν_c reduces the value of the ratio $\text{Im}(W_{10})/\text{Re}(W_{10})$ and therefore τ_{eff} ; in fact, the maximum practical value of ν_c would be set by the duration of the pulses in the three electromagnetic modes and the experimental convenience of accurately measuring the detuning. However, when the pure dephasing terms γ_{10} and γ_{30} are finite, τ_{eff} reaches a minimum for a finite value of ν_c . We assume that the dephasing rates are small enough that $\gamma_{10}, \gamma_{30} \ll \gamma_{20}, \gamma_{40}, |\Omega_b|, |\Omega_c|$. Therefore, substituting Eq. (2) into Eq. (3), we obtain

$$\nu_c = \left[\frac{\tilde{\gamma}_{20} (\gamma_{10}\tilde{\gamma}_{20} + |\Omega_a|^2)}{\tilde{\gamma}_{10}} \right]^{\frac{1}{2}} \frac{Q_c^2}{Q_b^2} \quad \text{and} \quad \tau_{\text{eff}} = 2 \left[\tilde{\gamma}_{10}\tilde{\gamma}_{20} (\gamma_{10}\tilde{\gamma}_{20} + |\Omega_a|^2) \right]^{\frac{1}{2}} \frac{Q_b^2}{|\Omega_b|^2} \frac{Q_c^2}{|\Omega_c|^2} \frac{\phi}{|\Omega_a|^2}, \quad (4)$$

where

$$Q_b^2 \equiv \gamma_{20}\gamma_{30} + |\Omega_b|^2, \quad Q_c^2 \equiv \gamma_{30}\gamma_{40} + |\Omega_c|^2, \quad \tilde{\gamma}_{10} \equiv \gamma_{10} + \gamma_{30} \frac{|\Omega_a|^2}{Q_b^2}, \quad \text{and} \quad \tilde{\gamma}_{20} \equiv \gamma_{20} + \gamma_{40} \frac{|\Omega_b|^2}{Q_c^2}. \quad (5)$$

Consider the case of a π phase gate, and assume that the pure dephasing rates are small enough that $\gamma_{20}\gamma_{30} \ll |\Omega_b|^2$, $\gamma_{30}\gamma_{40} \ll |\Omega_c|^2$, and $|\Omega_a|^2 \ll |\Omega_b|^2$. We see immediately that we can have $\tau_{\text{eff}} \ll 1$ only if $\gamma_{10}\tilde{\gamma}_{20} \ll |\Omega_a|^2$, giving $\nu_c \approx \sqrt{\tilde{\gamma}_{20}/\tilde{\gamma}_{10}}(|\Omega_c|^2/|\Omega_b|^2)|\Omega_a|$ and $\tau_{\text{eff}} \approx 2\pi\sqrt{\tilde{\gamma}_{10}\tilde{\gamma}_{20}}/|\Omega_a|$. Now, if $\gamma_{20} \approx \gamma_{40}$, then we must have $\gamma_{10} \ll |\Omega_a|^2|\Omega_c|^2/\gamma_{20}|\Omega_b|^2$, which could be difficult to achieve in a realistic experiment. However, if we can embed the atomic system in a photonic crystal and suppress spontaneous emission from atomic state $|4\rangle$,[8] this requirement is eased considerably to $\gamma_{10} \ll |\Omega_a|^2/\gamma_{20}$.

In addition to the decoherence error, there is also an error introduced when the Fock state $|n_b\rangle$ is replaced by the coherent state $|\alpha_b\rangle$ with $\langle n_b \rangle = |\alpha_b|^2$. When dephasing can be completely neglected, Eq. (2) shows that $W_{10} \propto n_a n_c / n_b$, and it is clear that the gate performs a phase shift when there is a photon present in *both* modes a and c , and no phase shift when either is absent. However, mode b is driven by a coherent state, and an input coherent state will evolve according to[8]

$$|\psi(t)\rangle = e^{-\frac{1}{2}|\alpha_b|^2} \sum_{n_b=0}^{\infty} \frac{\alpha_b^{n_b}}{\sqrt{n_b!}} e^{-i n_a n_c \phi(t) |\alpha_b|^2 / n_b} |\{1\}, n_a, n_b, n_c\rangle, \quad (6)$$

where $\phi(t) \equiv \tilde{W}t$, $\tilde{W} \equiv N|\tilde{\Omega}_a|^2|\tilde{\Omega}_c|^2/\nu_c|\tilde{\Omega}_b|^2|\alpha_b|^2$, and $|\tilde{\Omega}_k| \equiv |\Omega_k|/\sqrt{n_k}$. Clearly, if $|\alpha_b| \gg 1$, then only terms with $n_b \approx |\alpha_b|^2$ make a significant contribution to the sum, and the phase can be approximately factored out as

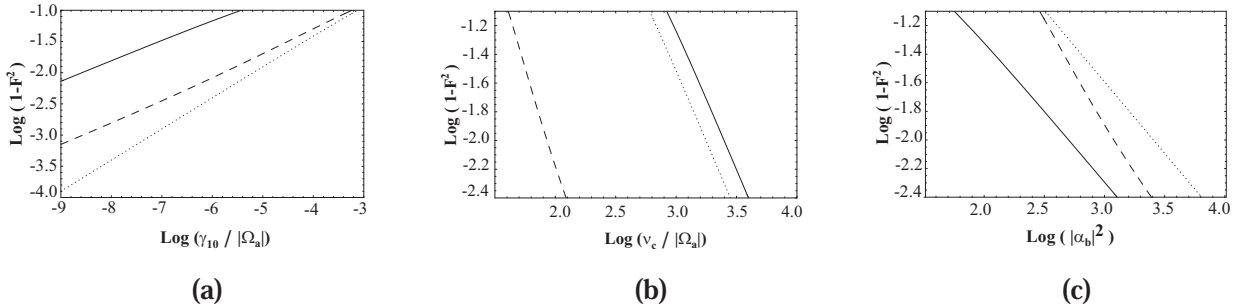


FIG. 2: The gate error as a function of (a) the logarithm of the dephasing, (b) detuning, and (c) coherent state intensity required to generate that error. In all plots, the solid lines (—) shows the error when emission from level $|4\rangle$ is not suppressed, i.e. $\gamma_{40} \sim \gamma_{20}$. The dashed lines (---) illustrates the case when γ_{40} has been suppressed relative to γ_{20} by a factor of 1000. The dotted lines (···) give the error in the case of the one-qubit phase gate when modes b and c are occupied by coherent states. In (c), the solid and dashed lines correspond to an ideal value of $|\alpha_b|$. However, the dotted line (···), shows a *minimum* value that $|\alpha_b|$ must take for the error in the one-qubit gate to remain below the value shown; $|\alpha_b|$ can take on larger values without affecting either the decoherence or the value of ν_c required to minimize the error. For the one qubit gate, $|\alpha_c| \gg |\alpha_b|$.

$|\psi(t)\rangle \approx e^{i\phi(t)}|1, n_a, \alpha_b, n_c\rangle$. However, if the coherent state is too weak, then the phase shift will be imperfectly implemented with a significant error, even in the absence of decoherence. Furthermore, we see from Eqs. (3) and (5) that the effect of the decoherence increases with the intensity of the coherent state, and therefore for a given dephasing there is some ideal value of α_b that minimizes the error.[9]

We are now ready to estimate the magnitude of the dephasing that must be achieved to obtain a given error. We assume that $|\Omega_a| \approx \gamma_{20}$ and $|\tilde{\Omega}_b|^2 \approx |\tilde{\Omega}_c|^2$, and we consider the most pessimistic case where $\gamma_{20} \approx \gamma_{40}$. We obtain

$$\frac{\gamma_{10}}{|\tilde{\Omega}_a|} = \left(\frac{\delta}{\phi}\right)^2 \frac{1}{n_b}. \quad (7)$$

This equation gives an estimate of the error arising from a *Fock* input state with an optimized value of ν_c for a particular level of decoherence. In Fig. 2(a) we plot the error induced on a *coherent* input state due to both decoherence and the finite intensity of the coherent state as a function of the dephasing γ_{10} , where we have chosen both ν_c and $|\alpha_b|$ to minimize the error. Figures 2(b) and 2(c) shows these values of α_b and ν_c chosen to give the largest possible dephasing for a given error.

As noted above, if γ_{40} can be suppressed, then the appropriate constraint $\gamma_{10} \ll |\Omega_a|^2/\gamma_{20} \approx \gamma_{20}$ becomes relatively easy to satisfy. For the requirement $|\alpha_b|^2 \ll \gamma_{40}/\gamma_{20}$, the dephasing can be larger than in the unsuppressed case by a factor of $|\alpha_b|^2$ and still produce the same error. By contrast, for $|\alpha_b|^2 \gg \gamma_{40}/\gamma_{20}$, the dephasing can be larger by a factor of γ_{40}/γ_{20} . Therefore, suppressing γ_{40} means that the detuning required is also much smaller.

In order to perform a two-qubit conditional phase gate with an error of 20% (and assuming we cannot suppress the depopulation from level $|4\rangle$), from Fig. 2 we find that the required parameters are $|\alpha_b| = 10$, $\nu_c/|\tilde{\Omega}_a| = 125$, and $\gamma_{10}/|\tilde{\Omega}_a| = 6 \times 10^{-7}$, and the gate operation time is determined by $|\Omega_a|Nt = 1.25 \times 10^4\phi$. However, if γ_{40} can be suppressed by a factor of 1000 relative to γ_{20} , the requirements are much reduced: the dephasing needed is $\gamma_{10}/|\tilde{\Omega}_a| = 2 \times 10^{-4}$, the detuning is $\nu_c/|\tilde{\Omega}_a| = 30$, and the coherent state must have $|\alpha_b| = 20$. The corresponding gate operation time is determined by $|\Omega_a|Nt = 160\phi$.

This system can also be used as a one-qubit phase shift gate (or an EIT-based QND detector,[9] where we can assume that $|\Omega_c| \approx |\Omega_b|$), *without* the extra effort described above for suppression of spontaneous emission from the atomic level $|4\rangle$. If mode c remains in the single-photon Fock state, the system will act as a phase shifter on mode a , and the above analysis applies. Alternatively, we can replace the quantum state in mode c with an intense coherent-state driving field. Now moderate (i.e., non-classical) values of $|\alpha_b|$ and $|\alpha_c|$ introduce errors. However, examining Eqs. (5), we see that—unlike for the two-qubit gate—the effects of decoherence depend much less sensitively on the intensities of the coherent states. As shown in Fig. 2, this means that we can eliminate the error due to the finite size of the coherent state, and we are only left with an error due to decoherence.

CONCLUSION

We have studied gates for quantum information processing based on a quantum treatment of EIT systems. We have analyzed in detail the performance of a two-qubit phase gate (and, by extension, that of a one-qubit phase gate) as functions of both atom and field properties, and we have described a general optimization method that selects a detuning that minimizes the gate error for a given phase shift. The resulting constraints on the allowable dephasing rates in these systems are quite stringent for high-fidelity operation. However, if the spontaneous emission rate from the atomic level $|4\rangle$ can be suppressed significantly, then demonstration of a moderate-fidelity phase gate becomes experimentally achievable.

* Electronic address: ray.beausoleil@hp.com

- [1] M. A. Nielsen and I. L. Chuang, **Quantum Computation and Quantum Information** (Cambridge University Press, 2000).
- [2] P. W. Shor, “Polynomial-Time Algorithm for Prime Factorization and Discrete Logarithms on a Quantum Computer,” Proc. 35th Annual Symposium on the Foundations of Computer Science, ed. S. Goldwasser, 124 (IEEE Computer Society Press, Los Alamitos, CA, 1994); SIAM J. Computing **26**, 1484 (1997); quant-ph/9508027.
- [3] L. K. Grover, “A fast quantum mechanical algorithm for database search,” Proc. 28th Annual ACM Symposium on the Theory of Computing (STOC), 212 (May 1996); quant-ph/9605043; Phys. Rev. Lett. **79**, 325 (1997); quant-ph/9706033.
- [4] S. Lloyd, “Universal Quantum Simulators,” Science **273**, 1073 (1996).
- [5] N. Gisin et al., “Quantum Cryptography,” Rev. Mod. Phys. **74**, 145 (2002).
- [6] H. Lee, P. Kok and J. P. Dowling, “Quantum Imaging and Metrology,” Proceedings of the Sixth International Conference on Quantum Communication, Measurement and Computing (QCMC02), edited by J. H. Shapiro and O. Hirota (Rinton Press, Paramus, New Jersey, USA, 2003), quant-ph/0306113..
- [7] K.-Y. Chen, T. Hogg and R. G. Beausoleil, “A quantum treatment of public goods economics,” Quant. Inf. Proc. **1**, 449 (2003); arXiv:quant-ph/0301013.
- [8] R. G. Beausoleil, W. J. Munro, and T. P. Spiller (2003), “Applications of Coherent Population Transfer to Quantum Information Processing,” J. Mod. Opt **51**, 1159 (2004); arXiv:quant-ph/0302109.
- [9] W. J. Munro, K. Nemoto, R. G. Beausoleil, and T. P. Spiller, “A high-efficiency quantum non-demolition single photon number resolving detector,” arXiv:quant-ph/0310066.
- [10] In Ref. [8], we explicitly required $|\Omega_a| \ll \gamma_{20}$ to obtain Eqs. 1 and 2. However, our subsequent numerical work has shown us that those results hold over a broad range of experimental parameters even when $|\Omega_a| \approx \gamma_{20}$.